Bulletin of the Seismological Society of America, Vol. 99, No. 2B, pp. 1215–1227, May 2009, doi: 10.1785/0120080247

Laboratory and Field Testing of Commercial Rotational Seismometers

by Robert L. Nigbor, John R. Evans, and Charles R. Hutt

Abstract There are a small number of commercially available sensors to measure rotational motion in the frequency and amplitude ranges appropriate for earthquake motions on the ground and in structures. However, the performance of these rotational seismometers has not been rigorously and independently tested and characterized for earthquake monitoring purposes as is done for translational strong- and weak-motion seismometers. Quantities such as sensitivity, frequency response, resolution, and linearity are needed for the understanding of recorded rotational data. To address this need, we, with assistance from colleagues in the United States and Taiwan, have been developing performance test methodologies and equipment for rotational seismometers. In this article the performance testing methodologies are applied to samples of a commonly used commercial rotational seismometer, the eentec model R-1. Several examples were obtained for various test sequences in 2006, 2007, and 2008. Performance testing of these sensors consisted of measuring: (1) sensitivity and frequency response; (2) clip level; (3) self noise and resolution; and (4) cross-axis sensitivity, both rotational and translational. These sensor-specific results will assist in understanding the performance envelope of the R-1 rotational seismometer, and the test methodologies can be applied to other rotational seismometers.

Introduction

Seismology and earthquake engineering both depend upon observation and measurement of earthquake-induced motion of the ground and structures. Both seismological and engineering measurements of earthquake motions focus on translational motions. However, rotational effects are observed in earthquakes, and both translational and rotational displacements are required to define motions of elements of the ground and components of structures (Teisseyre *et al.*, 2006). Rotational motion can be measured using multiple translational seismometers, as was reported by Niazi (1986) and Oliveira and Bolt (1989) and more recently by Spudich and Fletcher (2008) using dense array data from the 2004 Parkfield earthquake. However, in those studies and others it is acknowledged that such array measurement of rotations produces spatially averaged rotations that may not accurately represent point rotations.

Graizer (1991) recorded tilts and translational motions in the near field of two nuclear explosions using seismological observatory sensors to directly measure point rotations. Nigbor (1994) was the first to directly measure rotational and translational ground motions and observe significant amounts of rotational motions very near a large explosion using commercial rotational sensors. A commercial rotational velocity sensor from the aerospace field was used to directly measure the three rotational components of motion. This micro-electromechanical systems (MEMS)-based GyroChip gyroscopic sensor was well calibrated and characterized with metrology standards common in that field. The sensor was later deployed in the Borrego Valley in Southern California for an extended time but did not record any earthquake rotational ground motion above the sensor noise level. Takeo (1998) measured significant rotational motions very near some small earthquakes in Japan using a similar aerospace sensor, with similar issues of insufficient sensor resolution. Graizer (2006) presented results of large tilt measurements at Pacoima Dam during the 1994 Northridge earthquake inferred from translational accelerometer data but still representing point rotations.

These experiences, and similar experiences by other researchers, led to the need for rotational sensors with amplitude and frequency ranges more appropriate for strong-motion earthquake measurements on the ground and in structures. At the 2006 Workshop on Measuring the Rotation Effects of Strong Ground Motion (Evans *et al.*, 2007), it was generally agreed by the participants that the measurement of point rotational motions using existing and new sensors should be more widely investigated. This conclusion was echoed in the recommendations of the 2007 First International Workshop on Rotational Seismology and Engineering Applications (Lee *et al.*, 2007).

As the monitoring of rotational components of ground motion from earthquakes and explosions is further explored, it is critical to understand the performance of the available rotational seismometers. The same level of calibration and

performance testing currently applied to translation weak- and strong-motion seismometers should be applied to rotational seismometers (e.g., Hutt, 1990; Advanced National Siesmic System [ANSS] Technical Integration Committee, 2002; Institute of Electrical and Electronics Engineers [IEEE], 1998). This means that, in addition to the basic sensitivity and frequency response needed to convert sensor output to ground motion, overall sensor performance should be thoroughly characterized. The metrics of primary importance are: (1) sensitivity and frequency response; (2) clip level; (3) self-noise and resolution; and (4) cross-axis sensitivity, both rotational and translational. In this article, methods and facilities for such calibration and performance testing have been developed and applied to samples of a commonly used commercial rotational seismometer.

Rotational Sensors for Earthquake Monitoring

Rotational motion sensors are common in aerospace, automotive, and mechanical engineering where they are generically known as gyroscopic or inertial angular sensors. They can measure angular displacement, velocity (rate), acceleration, or jerk (rate of change of acceleration). They may or may not have response down to zero frequency.

IEEE (1985) provides generic specifications and performance test guidance for such inertial angular sensors. Primary performance tests are prescribed for frequency response (magnitude and phase), sensitivity, noise level, and cross-axis sensitivity (rotation and translation). These may be either static or dynamic tests. There are many other secondary tests discussed in the document.

Several angular sensor technologies have been adapted to the measurement of rotational components of earthquake motion on the ground and in structures. Fiber optic gyros (FOG) and ring laser gyros (RLG) have been used to measure low-amplitude, low-frequency rotational ground motions from earthquakes at regional and global distances (Igel *et al.*, 2007; Lee *et al.*, 2007). Both RLG and FOG sensors are expensive compared to traditional seismometers and so have had limited seismological applications to date.

MEMS-based Coriolis sensors were used by Nigbor (1994) and others to measure rotational components of strong ground motions. Nigbor (1994) details the theory of operation for this type of inertial sensor. Several currently available commercial angular sensors, including the ATA model ARS-9, PMD model RSB-20, and the eentec model R-1, use electrochemical technologies in which the motion of an electrolytic fluid inside a torus is sensed electronically, providing a voltage signal proportional to rotational velocity. It is these modest-cost commercial electrochemical sensors that, at this time, appear to have the most appropriate frequency and amplitude ranges for measurement of rotational motion from earthquakes at local and regional distances.

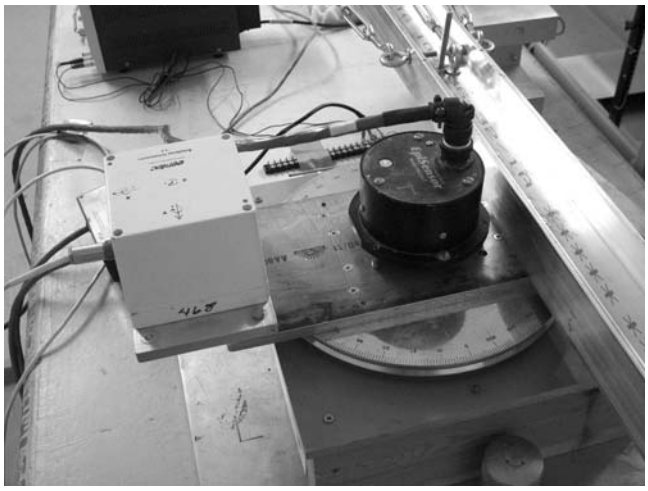

Figure 1. An R-1 rotational seismometer mounted on the USGS RST next to a triaxial translational accelerometer.

Of the commercially available angular sensors, the eentec model R-1 has been most extensively used for rotational earthquake and blast strong-motion measurements, for example, by Lin *et al.* (2009) for blast and earthquake measurements in Taiwan. Figure 1 shows a photograph of an R-1 installed on the rotational shake table (RST) discussed later in this article, adjacent to a common strong-motion accelerometer. There is a separate sensing element for each orthogonal Cartesian axis consisting of a toroidal cavity completely filled with an electrolyte. A microporous ceramic plug with four platinum electrodes is within each toroid. With angular velocity about the toroid axis a pressure differential is produced across the ceramic plug, causing the electrolyte to flow and current to flow across the electrode grid.

Table 1 lists the performance specifications for this triaxial rotational velocity sensor from eentec (2008). Figure 2

Table 1
eentec R-1 Performance Specifications (eentec, 2008)

Performance Metric	Units	Specified Value
Sensitivity	volts/radian/second (V/rad/sec)	50
Bandwidth	hertz	0.05–20 (0.03–50 optional)
Hard-clip level	rad/sec	0.05 (0.1 optional)
Maximum output	volts	±2.5 (±5 optional)
Self-noise level	rad/sec	$< 10^{-6}$ rms, 0.05–20 Hz
Resolution	rad/sec	1.2×10^{-7}
Linear cross axis	rad/sec per m/sec /sec	Not specified
Rotational cross axis	percent	Not specified

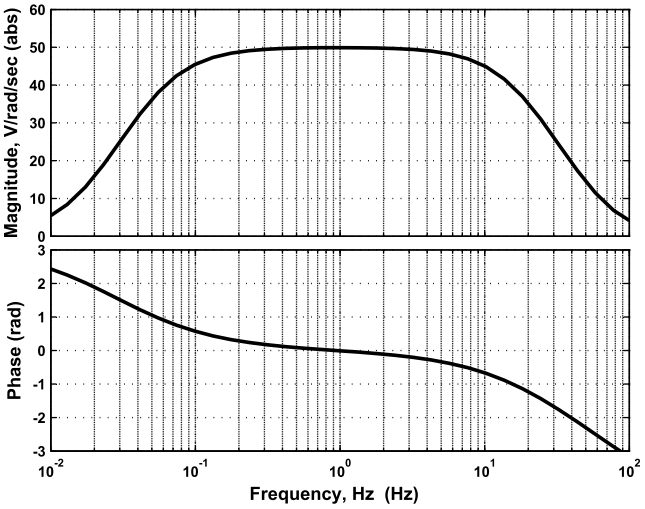

Figure 2. Nominal frequency response magnitude and phase for the R-1 (0.05–20 Hz version) and *S*-plane pole-zero model, both provided by eentec (2008).

shows the nominal frequency response magnitude and phase for the 0.05–20 Hz version of the R-1, derived from the manufacturer-provided pole-zero model of the frequency response in volts per radian per second given subsequently. The manufacturer states that the response of an R-1 will be within 1.5 dB of this nominal frequency response.

$$W(\omega) = \frac{A_0\omega^2}{[(s-p_1)(s-p_2)(s-p_3)(s-p_4)(s-p_5)]}, \quad (1)$$

where

- $A_0 = 1.669 \times 10^9$ [(rad/sec)^3 × v/(rad/sec)],
- ω = circular frequency,
- $s = j\omega$ = complex frequency,
- $z_1 = z_2 = 0$ (trivial zeros),
- $p_1 = 0.13$ rad/sec (0.02 Hz),
- $p_2 = 0.25$ rad/sec (0.04 Hz),
- $p_3 = 144$ rad/sec (23 Hz),
- $p_4 = 408$ rad/ sec (65 Hz), and
- $p_5 = 565$ rad/sec (90 Hz).

Some performance testing of the R-1 has previously been reported by Nigbor and Lee (2006). This testing included both laboratory and field testing, including sensitivity and cross-axis testing attempted on an engineering shake table. Difficulties were encountered in the fidelity of the shake table motions, and a conclusion was that better linear and RST facilities are needed to test the R-1 performance. Lin *et al.* (2009) describe calibration testing of seven R-1s using a precision tilt table to measure average sensitivity. Their results showed large deviations from the factory-specified sensitivity value, with as much as 30% difference between measured and nominal sensitivity. This result also points to the need for a more thorough performance testing of the R-1, in particular, and rotational seismometers, in general.

There is also concern, as with all seismic instruments, for sensor performance stability over the sometimes severe environmental conditions and the long time periods typical for earthquake observation. IEEE (1985) provides useful guidance on evaluation of environmental effects and short- and long-term stability of inertial angular sensors. While the results in this article do not directly address this important issue, it is noted that all of the performance parameters can be affected by the environment and can change over time.

Laboratory Testing of the R-1

Test Facility

Preliminary R-1 testing reported by Nigbor and Lee (2006) was done in laboratory and office settings at the University of California Los Angeles (UCLA) and at a remote field site in Southern California. The urban setting was not quiet enough for good noise measurements, and the engineering shake table at UCLA did not have the fidelity for R-1 performance testing. As a result, testing in 2007 and early 2008 was done at the U.S. Geological Survey's (USGS's) Albuquerque Seismological Laboratory (ASL) in New Mexico. ASL has existing facilities for testing seismom-

Figure 3. Seismic monitoring tunnel at ASL. Two R-1s are on the floor undergoing noise testing. Other covered instruments are reference broadband seismometers. The Q330 digitizers are on the floor to the right.

eters, has considerable experience with test methods, and is available for scientific sensor testing.

Two existing ASL capabilities and one new apparatus were used for the R-1 testing. The existing seismic monitoring tunnel provided a seismically quiet site for sensor noise testing, and an existing precision shake table was used for cross-axis response testing. A new RST was built specifically for rotational seismometer testing.

Figure 3 shows part of the seismic monitoring tunnel at ASL. This is a very quiet and stable site used for both continuous seismic monitoring and for noise testing of seismic instrumentation. This tunnel has power, communications, timing, and well-calibrated broadband seismometers to measure the seismic noise environment.

Figure 4 shows the precision horizontal shake table at ASL. This is a purpose-built horizontal shake table with a test platform measuring 60 by 73 cm and capable of supporting a test load up to 50 kg. It was designed and built in the mid-1990s by the Union Scientific Research Institute (UNIIA) of the USSR Ministry for Atomic Power Engineering and Industries in collaboration with the U.S. Geological Survey. The test platform is supported by four 50 cm radius arms, one at each corner, arranged as inverted pendulums. The lower end of each arm is connected to the base of the frame with cross flexures. The upper end of each arm is also connected to the test platform with cross flexures. The test platform therefore moves through an arc of 50 cm radius but remains horizontal within the error of the suspension arm lengths. The moving platform is driven by eight voice coils and has a useful displacement range of 20 mm peak-to-peak. The original design included driver electronics with feedback, but the feedback electronics failed after a few years of use and have not been replaced. Without feedback, the suspension has essentially zero restoring force, which means that it falls to one side or the other of its travel range. To overcome this problem, four tension springs have been installed between the frame and suspension (one on each suspension arm) to keep the suspension centered. With no test load, this results in a natural frequency of about 1.5 Hz. The table is driven by the voice coils through the use of a commercial low-distortion signal generator and direct current audio power amplifier. The result is a very quiet shake table able to produce nearly pure sinusoidal motion with very low

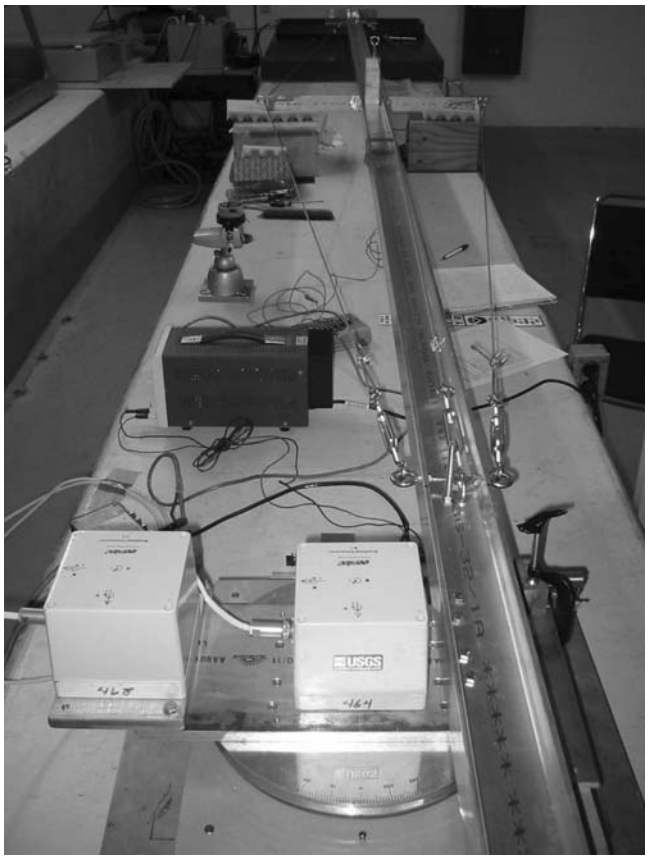

Figure 5. RST at ASL in the long-arm configuration. Two R-1s are mounted on the turntable, one centered and one off axis.

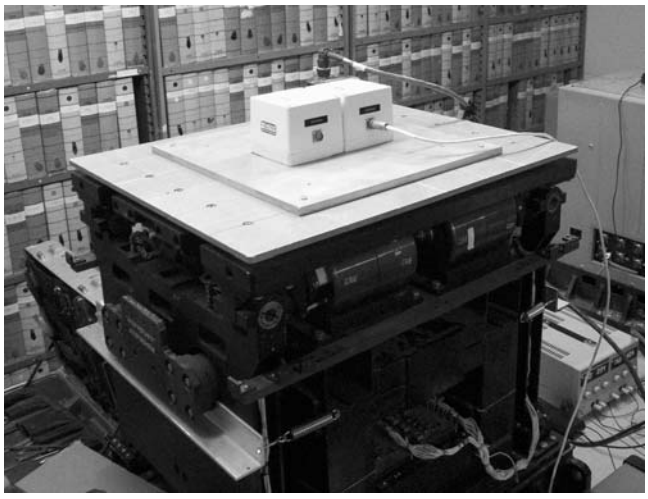

Figure 4. Russian-built precision shake table at ASL. Two R-1s are mounted on the table for cross-axis testing.

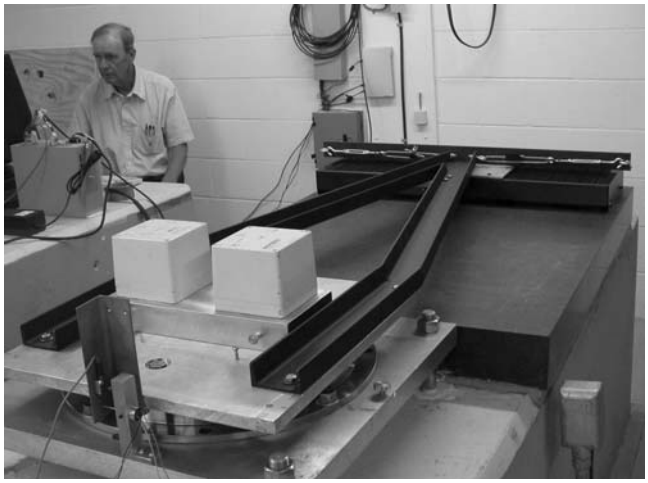

Figure 6. RST at ASL in the short-arm configuration. Two R-1s are mounted on the turntable, and the reference displacement and acceleration sensors can be seen in the foreground.

off-axis horizontal excitation at right angles to the main direction of motion. Previous tests show that the horizontal off-axis motion is about 60 dB below the on-axis motion. Because the suspension moves along an arc, there is some off-axis motion in the vertical direction at double the frequency of the drive signal.

Preliminary attempts to measure sensitivity and frequency response of rotational seismometers using tilt tables, step calibrators, or turntables were of limited value because of the high sensitivity of the R-1 and other similar sensors. It was clear that a precision RST was needed for accurate measurements of rotational seismometer performance. Our initial design coupled a precision aluminum turntable to a Rockwell/Anorad horizontal positioning stage (horizontal shake table) using a long truss beam as shown in Figure 5. Precision linear displacement of the positioning stage is then converted to precision rotation of the turntable. The initial beam length was 5.15 m. The maximum stroke of the positioning stage was ± 0.2 m and the position encoder of the system had a resolution of 0.1 μm, allowing very high precision control for both step and sine displacements. The nominal frequency range of the stage was 100 Hz, with displacement and force limits dictating the combined frequency and amplitude ranges.

With the long-arm configuration the arm had a fundamental vibration mode at about 20 Hz. This limited the usable frequency range of the table to about 15 Hz. A short-arm configuration, shown in Figure 6, had a much shorter (1.33 m) and stiffer arm configuration and a heavier turntable assembly. Tests show a fundamental vibration mode of this system at about 80 Hz, for a much broader usable frequency range to about 50 Hz.

In addition to measuring the control displacements at the drive end of the arm and dividing by the arm length to get angular displacements, rotational motion of the turntable was also measured directly using both an accelerometer and a displacement sensor (linear variable displacement transducer) for redundancy, both offset by about 0.1 m. For sinusoidal motion of the positioning stage, the measured rotational velocity of the turntable shows little distortion to the sinusoidal motion, less than 1% at frequencies below about 10 Hz. There is some rattle and off-axis motion that increases this distortion at higher frequencies, but the acceleration and displacement sensors on the turntable allow accurate rotational motion characterization.

In addition to the facilities mentioned previously, considerable instrumentation was needed for the R-1 testing. This included reference sensors, 24- and 26-bit dataloggers, and other electronic test equipment.

Testing Overview

Laboratory testing of R-1 performance was done in late 2007 and early 2008 at ASL. This testing built upon the earlier experience documented in Nigbor and Lee (2006).

In the 2007 testing, two R-1 samples, serial numbers 464 and 468, were subjected to the testing summarized in the test

Table 2
Performance Test Matrix, 2007 Test Sequence

Test Identification	Description	Performance Area				
		Gain	Frequency Resolution	Cross Axis	Linearity	Resolution
T1	Noise measurements in ASL tunnel. Two R-1s on concrete floor, input to Q330HR, overnight measurements of 6 channels at 200 samples/sec.					X
T2	Blast measurements in ASL tunnel. Locate two R-1s next to broadband reference sensor in tunnel. Monitor blast on 8/31 a.m.					X
S0	Characterize RST response to sine and square, and white noise.					
S1	Basic sensor gain for *z* axes using RST, 1 Hz sine at five amplitudes, for two R-1s (one centered, one offset).	X		X	X	
S2	Gain vs. frequency using RST, low-amplitude sine at 0.125, 0.25, 0.5, 1.0, 2.0, 4.0, 8.0, 10.0, 16, and 32 Hz, for two R-1s	X	X	X		
S3	Rotational cross axis using RST, 1 Hz sine at two amplitudes, one centered R-1, and spectrum analyzer analysis.			X		
S4	Broadband gain measurement using RST, two R-1s, and random excitation. Record on Q330HR.	X	X	X		
S5	Detailed sensor gain and cross axis using RST, 1 Hz sine at five amplitudes, and Q330 recording for two R-1s (one centered, one offset), *z* axis only	X		X	X	
S6	Linear cross axis using Russian linear shake table, two R-1s, Q330 recording.			X		
S7	*x*- and *y*-axis sensor gains using RST, 1 Hz sine at five amplitudes, for one R-1 on an angle bracket.	X		X	X	
S8	Rotational cross axis using RST, *x* and *y* axis, 1 Hz sine at two amplitudes, one centered R-1 on angle bracket.			X		
S9	Episensor rotational cross axis using RST, one ES-T centered, and one R-1 offset, 1 Hz, two amplitudes.			X		

matrix shown in Table 2. This testing included the measurement of self noise and blast motions in the ASL tunnel and nine different tests using either the RST (with long arm) or the precision horizontal shake table.

Testing in 2008 was a repeat of some of the RST testing using a short-arm configuration in an attempt to extend the usable frequency range to higher frequencies. R-1 serial numbers 468 and 123 were the two samples tested in this sequence. Additional clip level testing was done later in 2008 using R-1 serial number 561.

Test procedures and results are discussed in the sections following: Sensitivity and Frequency Response, Clip Level, Self Noise and Operating Range, and Cross-Axis Sensitivity.

Sensitivity and Frequency Response

Frequency response for a rotational seismometer is the complex transfer function between output voltage and the input case rotational velocity. This is typically measured in terms of amplitude and phase spectra, as shown in Figure 2 for the standard 0.05–20 Hz R-1. For seismometers, the measured frequency response is usually modeled in the Laplace domain with a best-fit pole-zero model. Figure 2 shows the nominal model provided for the R-1.

Sensitivity is the basic scalar value used to convert measured voltage output to motion units. For a sensor with a flat frequency response the sensitivity corresponds to a midfrequency average of the frequency response magnitude. For rotational seismometers sensitivity has units of volts per radian per second (V/rad/sec).

Bandwidth is defined as the portion of the frequency response magnitude spectrum that is flat in some sense. The definition is often the frequency band between the upper and lower frequencies where the magnitude falls 3 dB below the maximum value (called the −3 dB points). For the nominal R-1 frequency response in Figure 2, this bandwidth is 0.05–20 Hz.

The RST at ASL was used to measure these three quantities (frequency response, sensitivity, and bandwidth) for the vertical (z) axes of two R-1 samples. This was done by controlling the frequency and displacement of the horizontal positioning stage driving the RST in frequency steps from 1 to 50 Hz, with the displacement amplitude decreasing by $1/f$ to keep a constant velocity. Dwell at each frequency step was about 30 sec, enough for the RST and sensor to reach steady-state response.

Figure 7 shows sample time series data from the 2008 frequency response testing of R-1 serial number 468. This

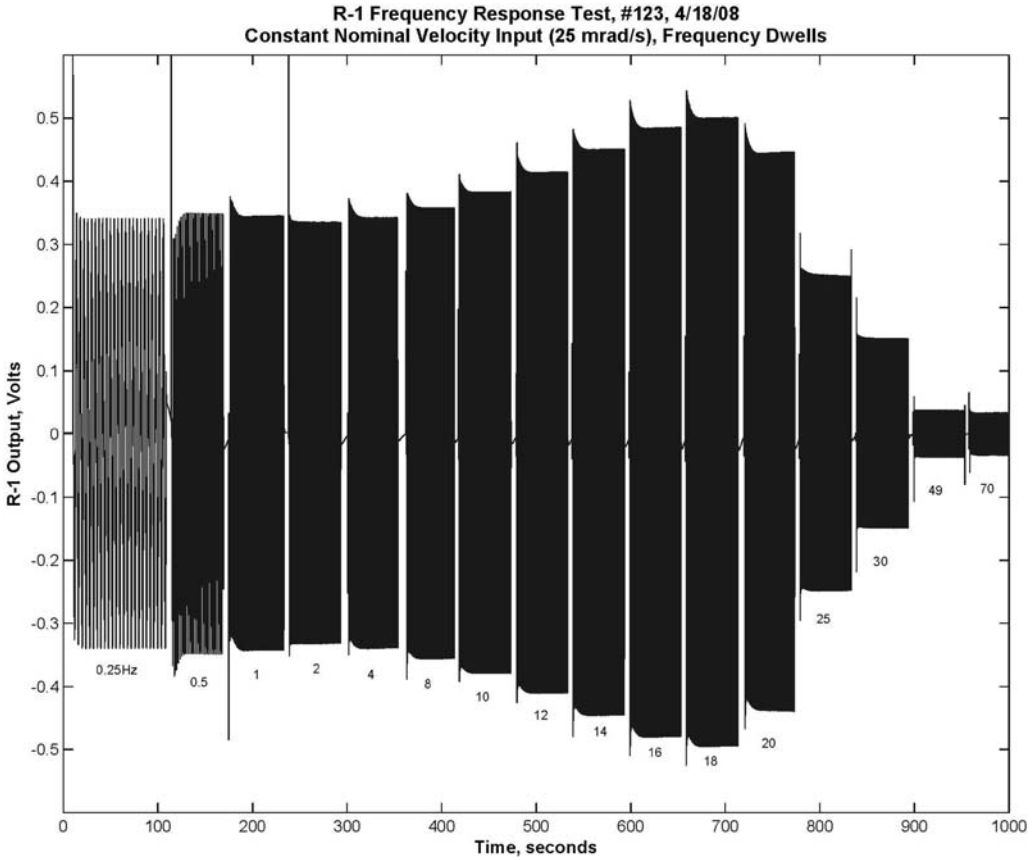

Figure 7. Sample frequency response test data for R-1 serial number 123, z axis. Dwell frequencies are noted for this constant nominal rotational velocity (2.5 mrad/sec) test. Note that actual rotational velocity input is directly measured and is different than nominal above 15 Hz due to arm response.

time series contains dwells at 14 frequencies from 1 to 50 Hz. Only the 2008 data were used to calculate frequency response, as the 2007 data were influenced by the long arm's vibrations at frequencies above 10 Hz.

For each dwell, the ratio between RST amplitude (rotational velocity, as measured using the horizontal positioning stage amplitude divided by the arm length and verified by both the turntable displacement and acceleration sensors as appropriate) and the R-1 output voltage was calculated to get the frequency response magnitude. The most robust way to get this magnitude was to evaluate the transfer function in the frequency domain at the shaking frequency, although other methods generally gave similar results when the sine signals were clean. The transfer function phase was measured at each frequency dwell by evaluating the transfer function phase in the frequency domain.

Figure 8 plots the measured transfer function magnitude and phase for R-1 serial number 123. Also plotted is

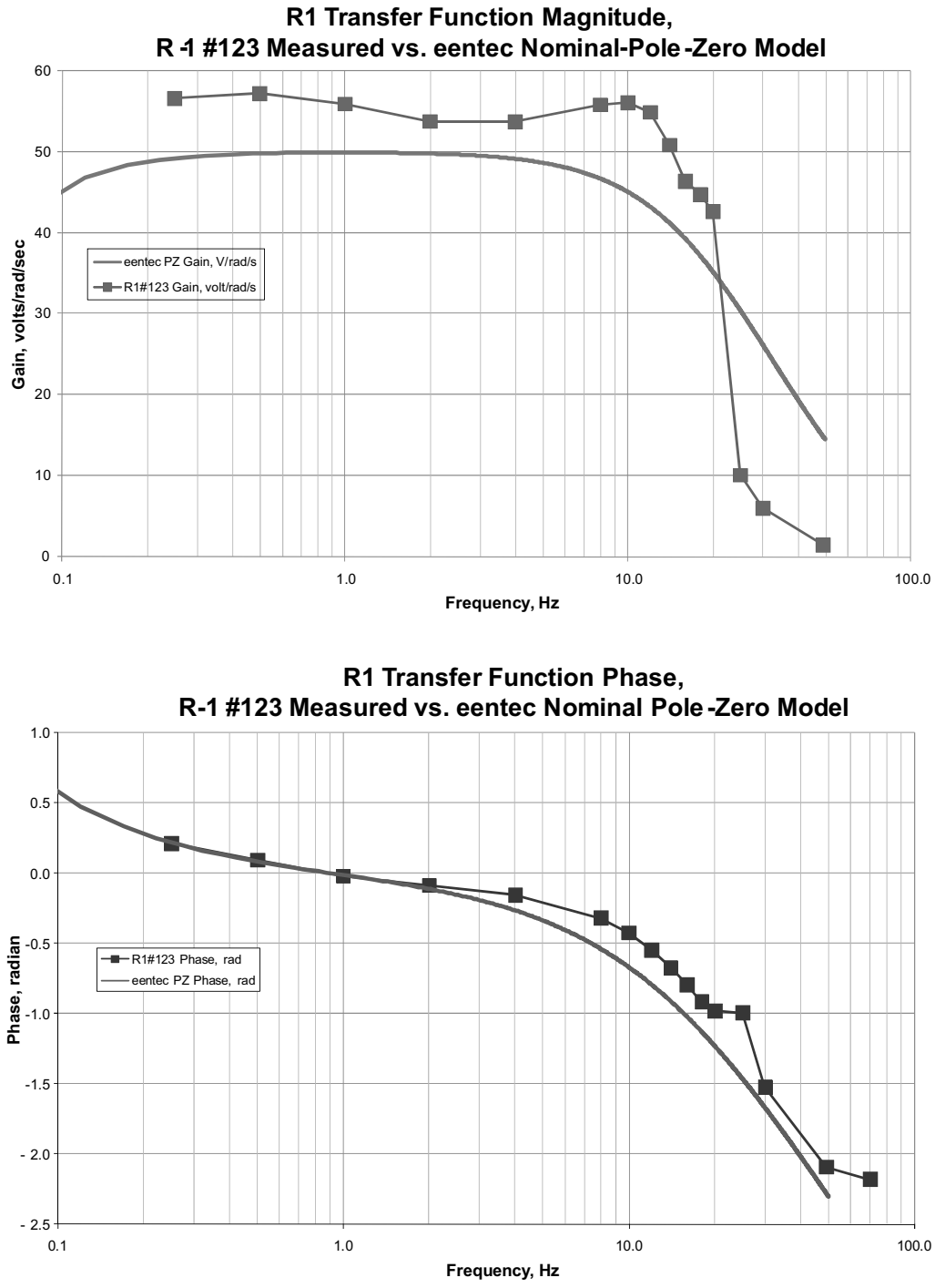

Figure 8. Measured and nominal pole-zero model frequency response magnitude and phase versus frequency for R-1 serial number 123.

Table 3
Measured R-1 Sensitivities and Upper Bandwidth Corners

R-1 Serial Number	4 Hz Sensitivity (V/rad/sec)	Upper Bandwidth Corner (Hz)
123	53.7	25
464	54.1	Not measured
468	51.7	23

the manufacturer-provided nominal pole-zero model transfer function for comparison.

The 4 Hz midband sensitivity values for the z axes of the three R-1s tested in 2007 and 2008 were calculated from the 4 Hz RST data in the various frequency response tests. These sensitivity values are shown in Table 3.

Bandwidth for an R-1 can be defined by finding the upper and lower frequencies at which the frequency response amplitude is 3 dB below the 4 Hz midband value. This definition is needed because of the nonflat nature of the in-band frequency response. This testing did not go low enough in frequency to measure the lower bound, but the upper bounds were estimated from frequency response data. Upper bandwidth corner frequencies for the z axes of two of the three sample R-1s are given in Table 3.

The RST and test procedures will be modified to accommodate all three sensor axes for future testing. Future work will also include the estimation of sensor-specific pole-zero models of the measured transfer function for use in sensor response correction.

Clip Level

Clip level is defined as the maximum output of a seismometer. A hard clip is defined as the maximum voltage output of a seismometer regardless of input. A soft clip is defined as the amplitude at which the output begins to be a distorted or nonlinear representation of the input waveform. For an ideal sensor the two clip levels are the same, with no distortion or nonlinearity before the hard clip is reached.

To measure both types of clipping for the R-1s, we mounted an R-1 on the RST and set the frequency to 1 Hz. Rotational amplitude was increased in steps until the nominal hard clip was reached. At each step sufficient time was allowed for the sensor to settle to a steady-state output. The time series for the z axis of the R-1s were analyzed qualitatively for amplitude and quantitatively for waveform distortion. Figure 9 shows an example of the clip level test data.

For the two R-1s tested, the soft-clip level occurred well below the nominal 2.5 or 5 V hard clip levels, with an average soft-clip level of about 75% of full scale at 1 Hz. These clip levels correspond to 0.04 rad/sec for the soft clip at 1 Hz

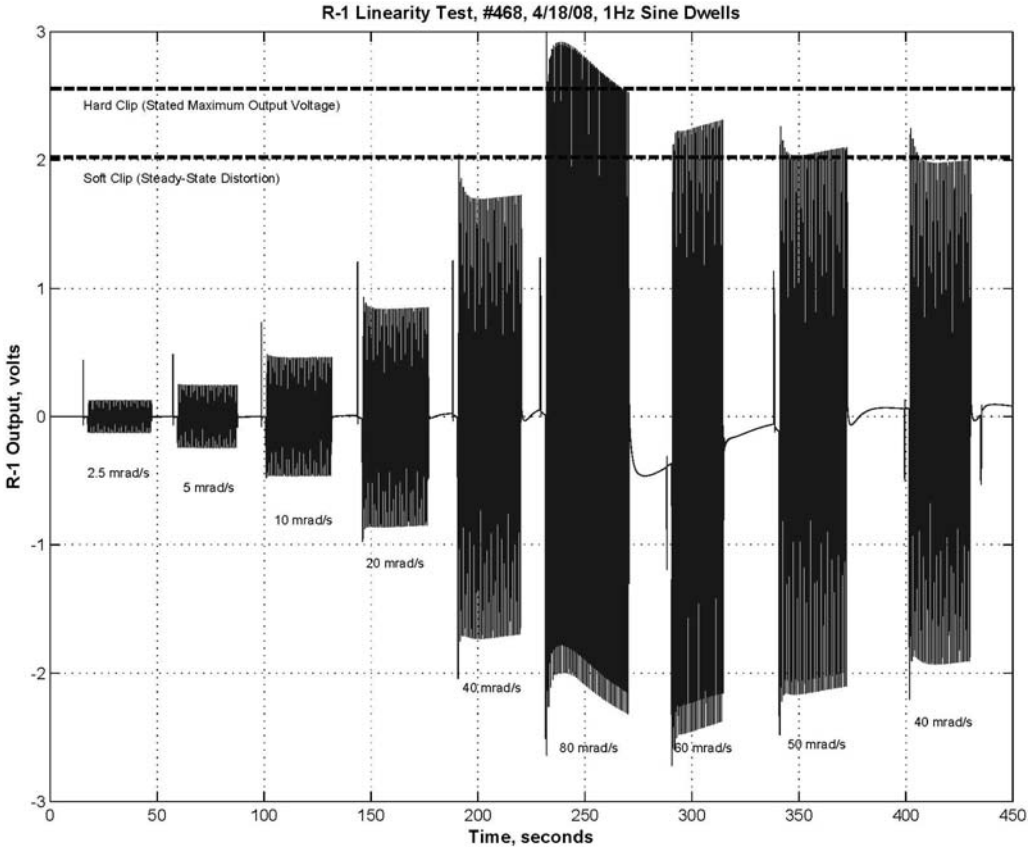

Figure 9. Sample clip level test data for R-1 serial number 468, z axis. Output voltage is plotted, and input rotational velocities are indicated for each 1 Hz sine dwell. Significant steady-state waveform distortion occurs above about 2 V peak output; transient distortion occurs at lower levels. Soft clip is 2 V at 1 Hz for this sensor, below the stated nominal hard-clip value of 2.5 V.

and 0.05 rad/sec for the nominal hard clip (for a 5 V maximum output sensor).

Additional testing was done in October 2008 on R-1 serial number 561 to further study the soft-clip phenomenon. The R-1 was placed on the RST, further modified to mount the R-1 in each of the three orthogonal axes. The excitation was set to 1 Hz, and the amplitude increased in steps until significant nonlinearity or distortion was observed in the steady-state waveform. This was repeated at 2, 4, 8, and 14 Hz. Frequency dependence was observed in the soft-clip level on all three axes, with nonlinearity occurring in the output at lower levels with increasing frequency. These results were used to develop the soft-clip level shown in the operating-range diagram discussed in the next section. It is clear from these tests that the R-1 clip level behavior is complex and should be characterized for each sensor. This soft-clip behavior should be considered when evaluating data from an R-1.

It was also observed throughout the testing that the sensors require several minutes to stabilize from a hard clip, such as when the sensor is moved or tilted. This behavior may limit the usefulness of the R-1 for large earthquake motions.

Self Noise and Operating Range

Self noise is defined as the electronic and mechanical noise at the output of a seismometer in the presence of zero input ground motion. Alternately, self noise is the portion of a seismometer output signal not related to ground or case motion. Evans *et al.* (2006) contains a more detailed definition and methodologies for measurement and analysis. Self noise of a seismometer is typically measured at a seismically quiet site using a single sensor (if sensor noise is higher than seismic noise) or two or three sensors (if the sensor's self noise is below seismic noise).

The seismic monitoring tunnel at ASL is a very seismically quiet site, with seismic noise well below the self noise of the R-1. Therefore, we were able to measure R-1 self noise by simply installing the sensors in the ASL tunnel (as shown in Fig. 3), connecting them to a 26 bit datalogger, and recording the output overnight.

The recorded data were then analyzed using the frequency domain methodology in Evans *et al.* (2006) to produce the self-noise power spectra in Figure 10. Plotted are the individual noise spectra for all six channels (three axes each for two R-1 samples). Figure 11 plots the coherence as a function of frequency between pairs of channels with the same measurement axis (x, y, and z). A coherence value of zero means that the signals are statistically independent; these results prove that the self noise of the R-1 is well above seismic noise in the ASL tunnel; and therefore the single-channel method for self-noise analysis is valid.

The measured noise spectra are consistent in shape and amplitude. They all have a very sharp increase in noise at low

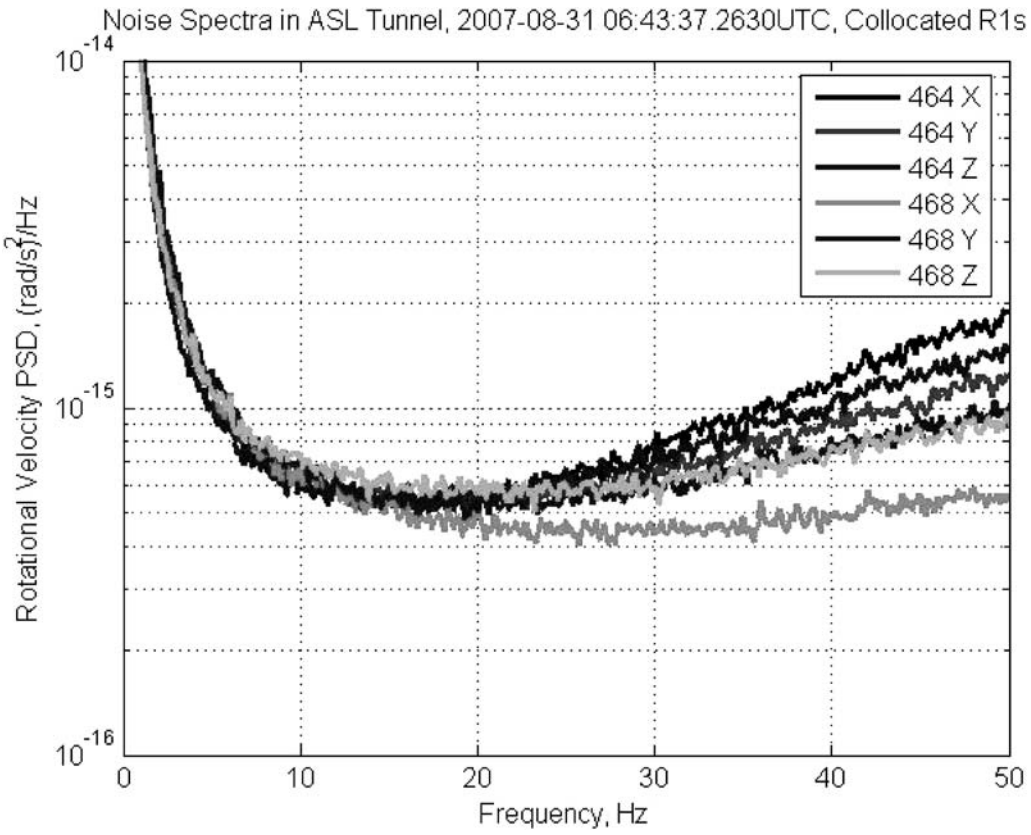

Figure 10. Measured self-noise spectra for all three axes of two R-1s.

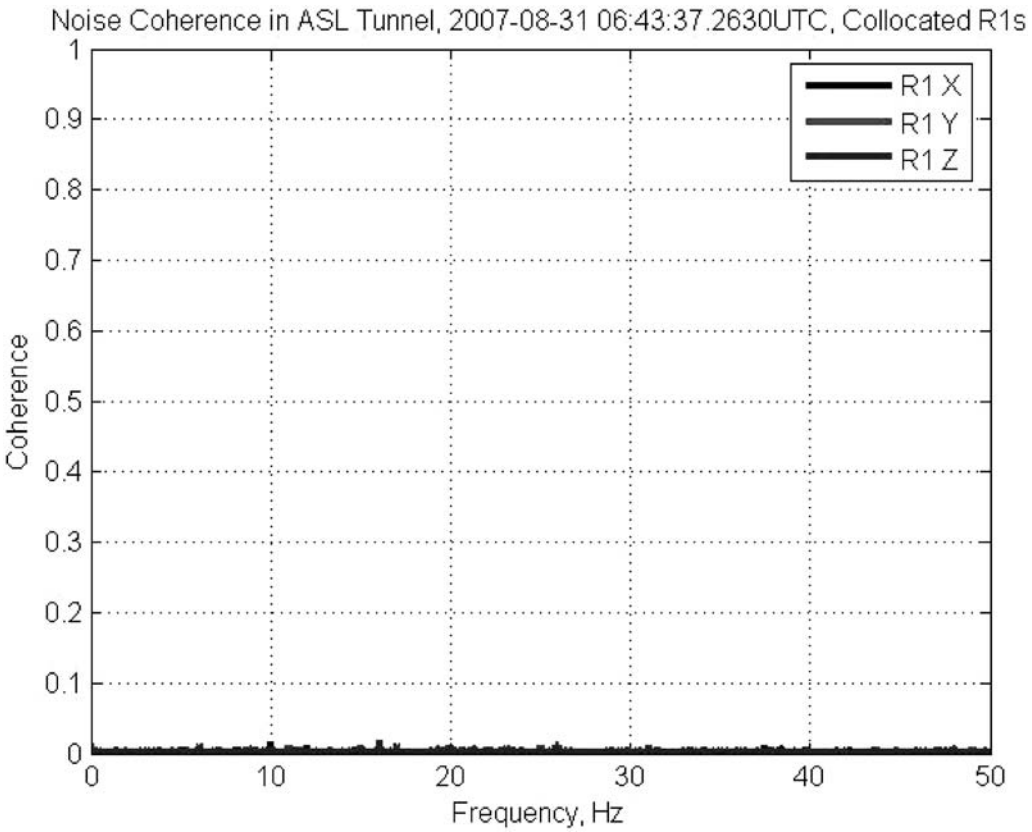

Figure 11. Noise coherence between a pair of R-1s in the ASL tunnel. Zero coherence means that the signal from each sensor is uncorrelated random noise, indicating that single-channel analysis of noise is valid.

frequencies, below about 5 Hz. The operating range of a sensor is defined as the portion of the ground-motion spectrum between the clip level and the self noise of a seismometer. Figure 12 is an operating-range diagram for the R-1 based upon test data herein. The plot includes the nominal hard-clip level as a frequency-independent constant value corresponding to the maximum stated voltage output of the sensor. It also includes a frequency dependent soft-clip level in the range 1–14 Hz derived from test data. Also on this plot, included for reference, are a collection of amplitude ranges from recorded rotational ground motions for blasts and earthquakes. These rotational motions are summarized by showing the frequency band over which they are above half the peak power of their power spectral density spectra and an amplitude equal to the time-domain peak rotational velocity (divided by $\sqrt{2}$ for comparison to the root mean square [rms] clipping level also shown in the figure).

At frequencies above 1 Hz, the difference between the clip level and self-noise level is roughly 4 orders of magnitude, or 80 dB, corresponding to about 14 bits of digital resolution. The operating range of the R-1 equates to roughly 12 bits resolution when so viewed.

Cross-Axis Sensitivity

Cross-axis sensitivity is defined for seismometers as the output of one axis resulting from motion inputs on orthogonal axes. Traditionally, cross-axis sensitivity for a translational seismometer only considers the two orthogonal translational axes. However, the general case should include both rotations and translations for a particular axis. Put another way, there will be five degrees of freedom contributing to the signal of any one axis through cross-axis sensitivity.

Cross-axis sensitivity is hard to measure precisely because of the off-axis errors in all shake tables and even in tilt tables. Therefore, a goal is to characterize it to one significant digit.

For the R-1s we have measured two types of cross-axis sensitivity: linear and rotational. Linear cross-axis sensitivity is the output of an R-1 axis due to linear acceleration in any of the three translational axes. Rotational cross-axis sensitivity is the output of an R-1 axis due to orthogonal rotational motion.

To measure linear cross-axis sensitivity we used the precision Russian-built shake table at ASL. Both an R-1 and a triaxial accelerometer (Kinemetrics model ES-T) were mounted on the shake table, and the table driven horizontally at 4.00 Hz and at maximum displacement, which produced a clean sine signal with $0.47g$ amplitude (4.7 m/sec/sec). Figure 13 shows sample data from this testing. The top three traces are the R-1 signals during this horizontal shaking. These signals are an unknown combination of linear cross-axis sensitivity and small rotations of the shake ta-

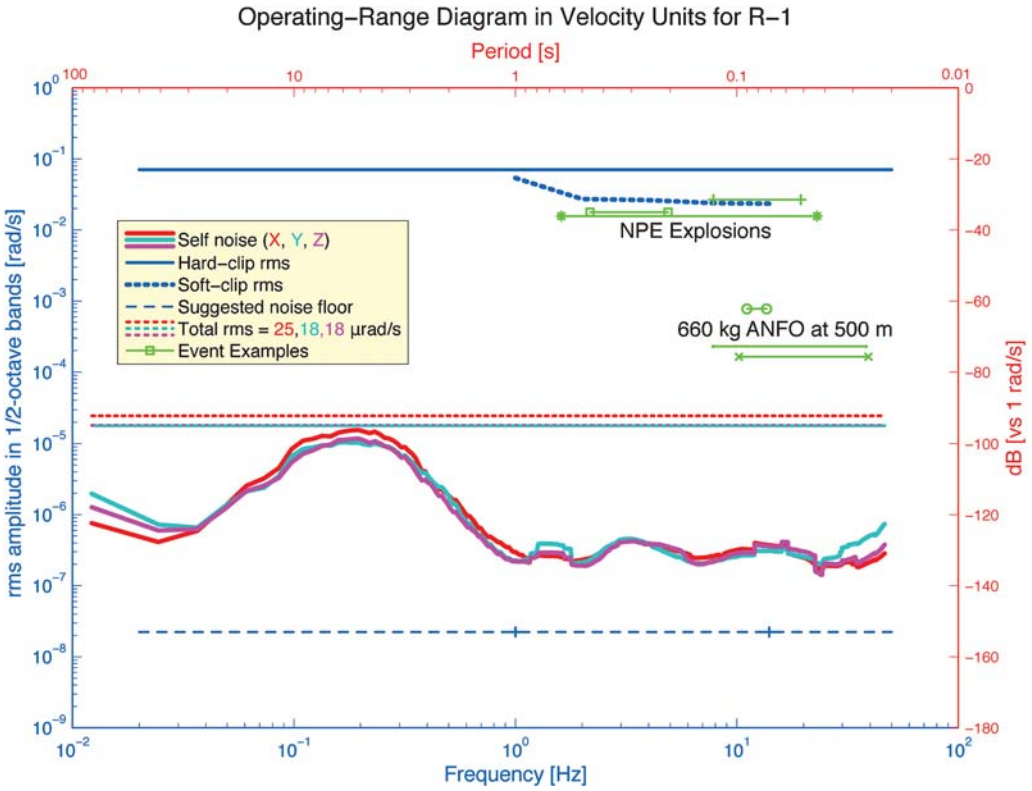

Figure 12. Measured R-1 operating range for R-1 serial number 464. The vertical scale is rms amplitude over 1/2-octave frequency bands. Measured hard- and soft-clip levels form the upper bound and self noise forms the lower bound of the range of this sensor. The event examples are provided for comparison only; these are a collection of blast and earthquake recordings of rotational ground motions.

ble, and so they represent a conservative estimate of the linear cross-axis sensitivity of the R-1. This testing was repeated for another R-1. The average peak signal of all six R-1 channels is 0.21 mrad/sec, and the maximum is 0.32 mrad/sec. This gives a conservative average linear cross-axis response of 0.04 (mrad/sec)/(m/sec^2) and a maximum of 0.06 (mrad/sec)/(m/sec^2).

For rotational cross-axis measurements the R-1 is mounted on the RST and shaken rotationally about its vertical (z) axis at 1 Hz. The signals on the two orthogonal axes are then measured. A conservative measure of rotational cross-axis sensitivity is the ratio between peak off-axis output to peak shake table rotation. Figure 14 shows sample rotational cross-axis data.

For the two sample R-1s, serial numbers 464 and 468, the rotational cross-axis sensitivity observed in these tests was about 2%. This is a conservative maximum value, as there are physical off-axis rotations of the RST due to mechanical looseness.

Conclusions

Calibration and performance testing of rotational seismometers presents difficult challenges not present in the testing of translational seismometers and accelerometers. Guidance and experience does exist in the aerospace community (IEEE, 1985, e.g.) for testing and calibration of the broad class of inertial angular sensors, but the frequency and amplitude ranges needed for measuring the rotational components of earthquake ground and structural motion present unique challenges. We have adapted test methods for translational seismometers and accelerometers to the investigation of rotational seismometers, focusing on sensor parameters of primary importance: sensitivity, frequency response, clip level, self noise and operating range, and rotational and translational cross-axis sensitivity. An RST was developed specifically for this testing at the U.S. Geological Survey's Albuquerque Seismological Laboratory.

Samples of a commercial rotational seismometer, the eentec model R-1, were tested using these methods and facilities to explore the performance of this sensor. The R-1, a fairly recent sensor using an innovative electrochemical technology, is responsible for much of the rotational ground motion recorded to date; therefore, this characterization is of importance to these new data sets. Test results show that the R-1 samples tested provide useful rotational data but that sensor-specific calibration should be considered to increase confidence. The nominal frequency response from the manufacturer-provided pole-zero model fits the measured transfer functions reasonably well as shown in Figure 8. The frequency and amplitude operating range shown in Figure 12 defines the useful performance range for earthquake monitoring of rotational ground and structural motions.

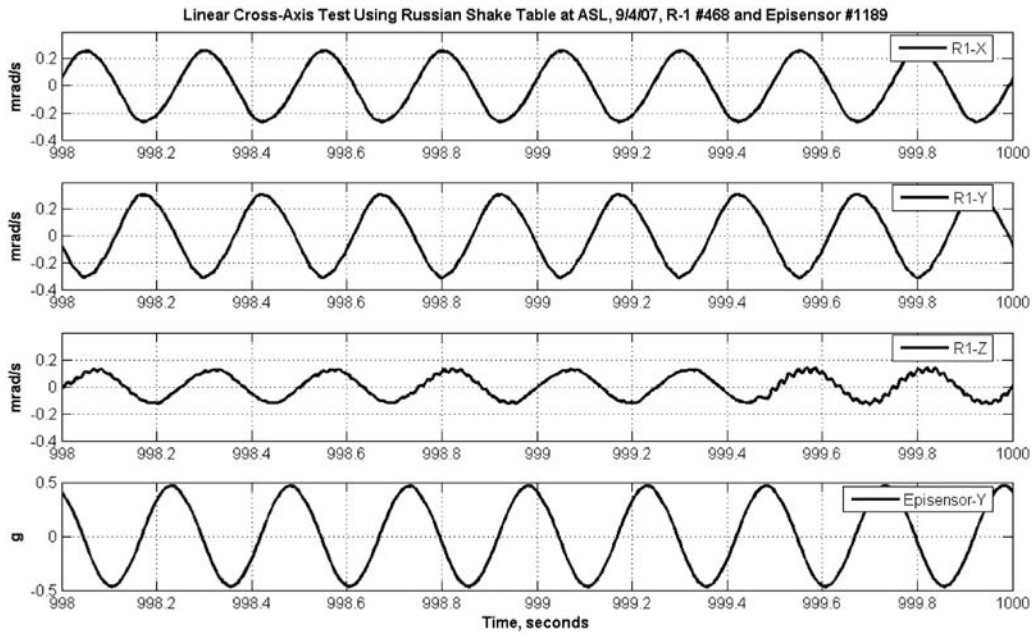

Figure 13. Linear cross-axis test data for R-1 serial number 468 for linear shaking in the *x* direction. Peak linear cross-axis response for this R-1 is 0.6 mrad/sec/g.

There are four findings that may adversely affect recorded data and should be considered by users of this sensor:

- There is significant variability in the sensitivity and frequency response, sometimes exceeding the 1.5 dB variability from the nominal transfer function stated by the manufacturer. It is recommended that individual calibration be performed for critical installations and sensors recording important data.
- The frequency response does not have the flat shape and linear phase commonly found in translational seismometers and accelerometers. Deconvolution of instrument response should be considered, especially when comparing translational and rotational data.

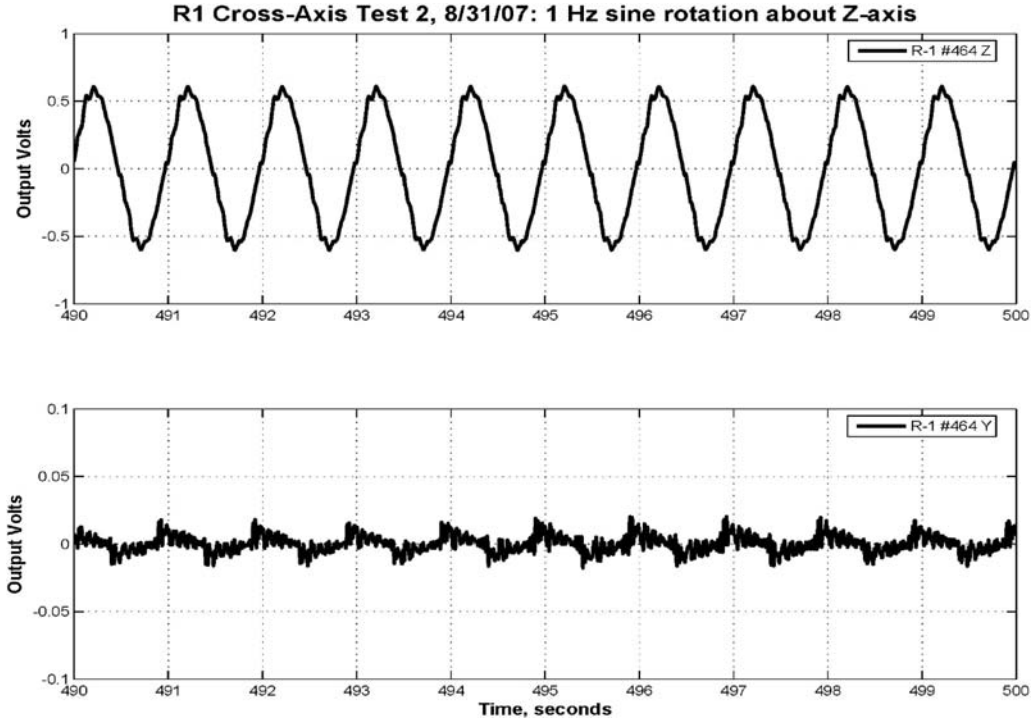

Figure 14. Sample rotational cross-axis test data for R-1 serial number 464.

- There is a soft clip observed in the sensor below the stated full-scale output. The sensor output becomes distorted and nonlinear at a decreasing voltage level as frequency increases. This soft clip should be considered as a limit of the operating range, as shown in Figure 12.
- Upon initial power on or after a hard clip, the sensor takes several minutes to recover to a stable baseline. This may affect data quality under very strong ground motions.

As a final comment, we are continuing to improve the facilities at ASL for testing of rotational seismometers and can make these facilities available to the scientific community for appropriate testing purposes.

Data and Resources

All of the data used in this study were collected by the authors. Most were collected using the facilities and equipment of the USGS ASL. Some were collected using equipment and facilities provided by the University of California at Santa Barbara (UCSB) and UCLA sites of the George E. Brown Jr. Network for Earthquake Engineering Simulation (NEES).

Acknowledgments

We wish to thank the many individuals involved in the International Working Group on Rotational Seismology for their encouragement of rotational earthquake motion measurements. In particular, Willie Lee has been a primary inspiration and a facilitator for our testing efforts.

Chuck Langston, Jamie Steidl, NEES@UCSB, and NEES@UCLA contributed equipment to these tests. Vernon Stoup was instrumental in the construction of the test facility at ASL. Chin Jen Lin assisted with data analyses.

Rob Abbott, Leo Sandoval, and two anonymous reviewers greatly improved the article through their careful review of the manuscript and results.

References

Advanced National Seismic System (ANSS) Technical Integration Committee (2002). Technical guidelines for the implementation of the advanced national seismic system—version 1.0, *U.S. Geol. Surv. Open-File Rept. 02-0092*, available at http://www.anss.org (last accessed August 2008).

eentec (2008). *Instruction Manual, Model R-1*, St. Louis, Missouri, 8 pp., available at http://www.eentec.com/ (last accessed August 2008).

Evans, J. R., A. Cochard, V. Graizer, B.-S. Huang, K. Hudnut, C. R. Hutt, H. Igel, W. H. K. Lee, C.-C. Liu, E. Majewski, R. Nigbor, E. Safak, W. U. Savage, U. Schreiber, R. Teisseyre, M. Trifunac, J. Wassermann, and C.-F. Wu (2007). Rotational seismology workshop of February 2006, *U.S. Geol. Surv. Open-File Rept. 2007-1145*, available at http://pubs.usgs.gov/of/2007/1145/ (last accessed August 2008).

Evans, J. R., R. L. Nigbor, and C. R. Hutt (2006). C-language software for computing strong ground motion metrics and self noise, *U.S. Geol. Surv. Open-File Rept. 2006-1369*.

Graizer, V. (2006). Tilts in strong ground motion, *Bull. Seismol. Soc. Am.* **96,** 2090–2106.

Graizer, V. M. (1991). Inertial seismometry methods, *Izv. USSR Acad. Sci, Phys. Solid Earth* **27,** no. 1, 51–61.

Hutt, C. (1990). Standards for seismometer testing—a progress report, available from Albuquerque Seismological Laboratory at http://www.earthquake.usgs.gov/regional/asl (last accessed August 2008).

Institute of Electrical and Electronics Engineers (IEEE) (1985). IEEE standard specification format guide and test procedure for nongyroscopic inertial angular sensors: jerk, acceleration, velocity, and displacement, *IEEE Std 671-1985*, Institute of Electrical and Electronics Engineers, New York, New York.

Institute of Electrical and Electronics Engineers (IEEE) (1998). IEEE standard specification format guide and test procedure for linear, single-axis, nongyroscopic accelerometers, *IEEE Std 1293-1998*, Institute of Electrical and Electronics Engineers, New York, New York.

Igel, H., A. Cochard, J. Wassermann, A. Flaws, U. Schreiber, A. Velikoseltsev, and N. Pham Dinh (2007). Broadband observations of earthquake-induced rotational ground motions, *Geophys. J. Int.* **168,** 182–196.

Lee, W. H. K, M. Çelebi, M. I. Todorovska, and M. F. Diggles (2007). *Proc. of the 1st International Workshop on Rotational Seismology and Engineering Applications*, Menlo Park, California, 18–19 September 2007, *U.S. Geol. Surv. Open-File Rept. 2007-1144*.

Lin, C.-J., C.-C. Liu, and W. H. K. Lee (2009). Recording rotational and translational ground motions of two TAIGER explosions in northeastern Taiwan on 4 March 2008, *Bull. Seismol. Soc. Am.* **99,** no. 2B, 1237–1250.

Niazi, M. (1986). Inferred displacements, velocities and rotations of a long rigid foundation located at El Centro differential array site during the 1979 Imperial Valley, California, earthquake, *Earthq. Eng. Struct. Dyn.* **14,** 531–542.

Nigbor, R. L. (1994). Six-degree-of-freedom ground motion measurement, *Bull. Seismol. Soc. Am.* **84,** 1665–1669.

Nigbor, R. L., and W. H. K. Lee (2006). A preliminary evaluation of the R-1 rotational sensor, a report posted online at: http://www.rotational-seismology.org/ (last accessed August 2008).

Oliveira, C. S., and B. A. Bolt (1989). Rotational components of surface strong ground motion, *Earthq. Eng. Struct. Dyn.* **18,** 517–526.

Spudich, P., and J. B. Fletcher (2008). Observation and prediction of dynamic ground strains, tilts, and torsions caused by the *M* 6.0 2004 Parkfield, California, earthquake and aftershocks, derived from UPSAR array observations, *Bull. Seismol. Soc. Am.* **98,** 1898–1914.

Takeo, M. (1998). Ground rotational motions recorded in near-source region of earthquakes, *Geophys. Res. Lett.* **25,** 789–792.

Teisseyre, R., M. Takeo, and E. Majewski (Editors) (2006). *Earthquake Source Asymmetry, Structural Media, and Rotation Effects*, Springer-Verlag, Berlin.

Department of Civil Engineering
UCLA
5731 Boelter Hall
Los Angeles, California 90095
nigbor@ucla.edu
(R.L.N.)

U.S. Geological Survey
345 Middlefield Road, MS-977
Menlo Park, California 94025
(J.R.E.)

U.S. Geological Survey
P.O. Box 82010
Albuquerque, New Mexico 87198-2010
(C.R.H.)

Manuscript received 22 August 2008